In vivo imaging of hydrogen peroxide production in a murine tumor model with a chemoselective bioluminescent reporter

Genevieve C. Van de Bittner[a], Elena A. Dubikovskaya[a], Carolyn R. Bertozzi[a,b,c,d], and Christopher J. Chang[a,b,1]

[a]Department of Chemistry, [b]Howard Hughes Medical Institute, and [c]Department of Molecular and Cell Biology, University of California, Berkeley, CA 94720; and [d]The Molecular Foundry, Lawrence Berkeley National Laboratory, Berkeley, CA 94720

Edited by Doug Neckers, Spectra Group Ltd., Millbury, OH, and accepted by the Editorial Board October 15, 2010 (received for review August 29, 2010)

Living organisms produce hydrogen peroxide (H_2O_2) to kill invading pathogens and for cellular signaling, but aberrant generation of this reactive oxygen species is a hallmark of oxidative stress and inflammation in aging, injury, and disease. The effects of H_2O_2 on the overall health of living animals remain elusive, in part owing to a dearth of methods for studying this transient small molecule in vivo. Here we report the design, synthesis, and in vivo applications of Peroxy Caged Luciferin-1 (PCL-1), a chemoselective bioluminescent probe for the real-time detection of H_2O_2 within living animals. PCL-1 is a boronic acid-caged firefly luciferin molecule that selectively reacts with H_2O_2 to release firefly luciferin, which triggers a bioluminescent response in the presence of firefly luciferase. The high sensitivity and selectivity of PCL-1 for H_2O_2, combined with the favorable properties of bioluminescence for in vivo imaging, afford a unique technology for real-time detection of basal levels of H_2O_2 generated in healthy, living mice. Moreover, we demonstrate the efficacy of PCL-1 for monitoring physiological fluctuations in H_2O_2 levels by directly imaging elevations in H_2O_2 within testosterone-stimulated tumor xenografts in vivo. The ability to chemoselectively monitor H_2O_2 fluxes in real time in living animals offers opportunities to dissect H_2O_2's disparate contributions to health, aging, and disease.

cancer | molecular imaging | redox biology

An emerging body of data indicates that hydrogen peroxide (H_2O_2) is a component of cell signaling pathways that are necessary for the growth, development, and fitness of living organisms (1–6). However, imbalances in H_2O_2 production lead to oxidative stress and inflammation events, which damage tissue and organ systems and are correlated with the onset and advancement of various diseases, including cancer (7, 8), diabetes (9, 10), and cardiovascular (11, 12) and neurodegenerative (13, 14) diseases. In this context, H_2O_2 is a key focus of research into the chemical mechanisms underlying the development and progression of disease.

The involvement of H_2O_2 in cellular signaling and disease states has motivated the construction of chemical tools to probe the complex contributions of this reactive oxygen metabolite to living systems by employing molecular imaging. Most of these small-molecule (15–21) and protein-based (22) reporters have been fashioned to operate as fluorescent indicators in dissociated cell culture specimens and small transparent animals like zebrafish, but strategies to visualize H_2O_2 fluxes in larger mammalian animals, such as mice, remain limited. In this regard, one elegant example of a chemiluminescent reporter for imaging H_2O_2 in mice using peroxalate-based nanoparticles has been described (23). These peroxalate nanoparticles exhibit high H_2O_2 selectivity and sensitivity and are effective for imaging hydrogen peroxide produced in the inflammatory response to lipopolysaccharide. However, this approach precludes detection of intracellular H_2O_2 because of the size of the first-generation nanoparticles, requires removal of fur and skin for signal detection from the tissue of interest, and cannot be used to simultaneously detect H_2O_2 in multiple regions or in the entire organism without injection of the nanoparticles at multiple sites.

To develop methods to meet the criteria of membrane diffusion and tissue penetration for whole-animal H_2O_2 detection, we chose bioluminescence as an imaging technique because of its favorable properties for in vivo imaging. In particular, bioluminescence resulting from the catalytic transformation of firefly luciferin by the firefly luciferase enzyme exhibits a high efficiency for photon production (24, 25) and a 612-nm emission, which result in a detectable bioluminescent signal in all organs of a mouse (26, 27). This modality also features small, membrane-diffusible substrates for intracellular detection of analytes and mobility of probes throughout the organism (26, 28), as well as a greater signal-to-noise contrast ratio compared to fluorescence, which allows for increased sensitivity to in vivo analytes (29). In this report, we present a chemoselective, bioluminescent reporter for H_2O_2 in living cells and mice. Peroxy Caged Luciferin-1 (PCL-1) (Fig. 1) is a small-molecule caged luciferin that possesses an H_2O_2-sensitive aryl boronic acid connected to the phenolic position of firefly luciferin through a self-immolative linker, which, upon reaction with H_2O_2, releases luciferin for subsequent reaction with the firefly luciferase enzyme to produce a photon (Fig. 1). We establish the ability of PCL-1 to detect H_2O_2 selectively and in a concentration-dependent manner in aqueous solution and in living cells and demonstrate the ability of PCL-1 to detect both extra- and intracellular H_2O_2. Moreover, subsequent studies with exogenous H_2O_2 and antioxidant treatment show that PCL-1 can visualize basal H_2O_2 levels as well as H_2O_2 fluctuations in all regions of living, luciferase-expressing mice (FVB-luc$^+$ mice) without removal of fur or skin. Finally, PCL-1 molecular imaging in living mice with LNCaP-luc xenograft prostate tumors reveals that LNCaP tumors respond to testosterone by producing H_2O_2 and that this oxidative burst can be diminished by treatment with the antioxidant *N*-acetylcysteine (NAC). Our findings presage the utility of PCL-1 as a powerful tool for studying the development and progression of diseases such as cancer, neurodegeneration, heart disease, and diabetes, which have all been linked to imbalances in H_2O_2 and related reactive oxygen species (ROS).

Author contributions: G.C.V.d.B., E.A.D., C.R.B., and C.J.C. designed research; G.C.V.d.B. and E.A.D. performed research; G.C.V.d.B. contributed new reagents; G.C.V.d.B. and E.A.D. contributed analytic tools; G.C.V.d.B., E.A.D., C.R.B., and C.J.C. analyzed data; and G.C.V.d.B. and C.J.C. wrote the paper.

The authors declare no conflict of interest.

This article is a PNAS Direct Submission. D.N. is a guest editor invited by the Editorial Board.

[1]To whom correspondence should be addressed at: Department of Chemistry, Room 532A Latimer Hall, University of California, Berkeley, CA 94720-1460. E-mail: chrischang@berkeley.edu.

This article contains supporting information online at www.pnas.org/lookup/suppl/doi:10.1073/pnas.1012864107/-/DCSupplemental.

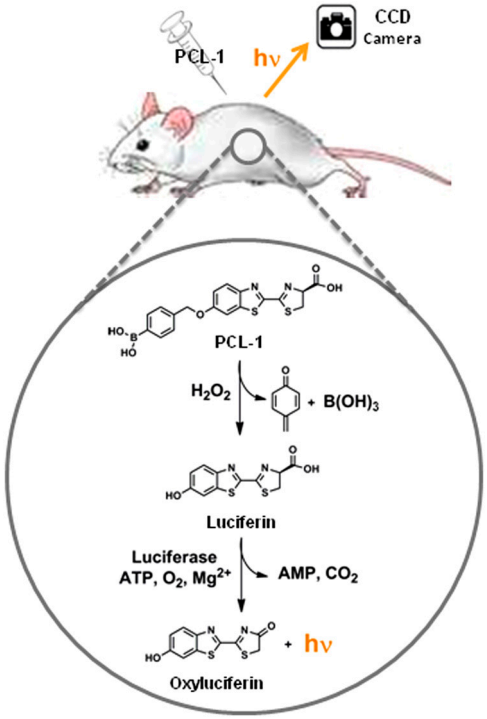

Fig. 1. Design strategy for H_2O_2-mediated release of firefly luciferin from PCL-1.

Results and Discussion

Design and Synthesis of PCL-1. Desirable properties for an effective H_2O_2 reporter in living animals include selectivity for H_2O_2 over other biologically relevant ROS, a good signal-to-noise contrast ratio, high-efficiency signal production, and deep tissue signal penetration. In addition, practical molecular imaging probes for use in whole organisms should be readily transported in vivo, minimally invasive, and nontoxic. We chose the firefly luciferin/luciferase bioluminescent reporter system as a platform for creating in vivo H_2O_2 imaging agents because it meets all of the aforementioned chemical and biological criteria. In particular, the firefly luciferin substrate is a nontoxic small molecule that easily enters the blood stream, produces tissue-penetrable signal in all organs of transgenic mice, and is metabolized within hours (30–32).

We envisioned a bioluminescent H_2O_2 reporter in which an appropriately caged firefly luciferin that is unreactive toward the luciferase enzyme could be unmasked by a selective H_2O_2-mediated cleavage process to generate free luciferin and subsequently trigger the catalytic bioluminescent luciferin/luciferase reaction. Related strategies have been employed for assaying enzyme activity (33–38) and cell-penetrating peptide transport efficiency (39), but these strategies have not been used for small-molecule detection. Alkylation of firefly luciferin at the phenolic position prevents signal production even when luciferin's reactive carboxylic acid moiety remains unaltered (40). Additionally, previous work from our laboratory has shown that the chemoselective deprotection of boronate esters to phenols offers a useful reaction-based method for detecting H_2O_2 over other ROS (16, 18–21, 41, 42). On the basis of these considerations, we designed the peroxide-sensitive probe PCL-1 (Fig. 1) by attaching an aryl boronic acid to firefly luciferin through a self-immolative benzylic linker (43–45). In the absence of H_2O_2, PCL-1 is not an active substrate for the luciferase enzyme, but addition of H_2O_2 triggers cleavage of the boronic acid benzyl ether to release free luciferin, which reacts with firefly luciferase to produce a bioluminescent readout. The synthesis of PCL-1 is depicted in Scheme 1.

Peroxide Reactivity and Selectivity of PCL-1. Initial experiments tested the kinetic properties of PCL-1 and the ability of PCL-1 to detect H_2O_2 in a selective and concentration-dependent manner. First, we performed an in vitro kinetic assay with PCL-1 (5 μM) and H_2O_2 (1, 5, and 10 mM) to determine the second-order rate constant ($k = 3.8 \pm 0.34\ M^{-1}\ s^{-1}$) for the reaction. Next, we evaluated the ROS selectivity of the reaction in a bioluminescent assay using purified firefly luciferase. PCL-1 was incubated with a panel of ROS, including H_2O_2 in the absence and presence of catalase, an H_2O_2-degrading enzyme, for 5–60 min followed by addition of firefly luciferase. Subsequently, light production was measured over 45 min to determine the relative amount of luciferin released during the ROS incubation period. The relative total photon flux for each condition was calculated by dividing the total photon flux for the experimental condition by the total photon flux for PCL-1 alone to allow a direct comparison between various ROS. Whereas addition of H_2O_2 showed a *ca.* sevenfold increase in bioluminescent signal over an hour, there was little to no increase in signal when the boroic acid probe was reacted with the other ROS or H_2O_2 in the presence of catalase (Fig. 2). Additionally, our control compounds, luciferin and valeryl luciferin, which were used for in vivo experiments, showed little to no response to incubation with ROS in vitro (Fig. S1).

After confirming the selectivity of PCL-1 for H_2O_2 over other biologically relevant ROS, we examined the responsiveness of PCL-1 to alterations in peroxide levels. Incubation of PCL-1 with various concentrations of H_2O_2 for 60 min was followed by addition of firefly luciferase and detection of the released luciferin through measurement of the bioluminescent signal. This assay established the linear dependence ($R^2 = 0.9927$) of luciferin release from PCL-1 on the concentration of H_2O_2 over a 2-order-of-magnitude range, from 5 to 250 μM (Fig. 2 and Fig. S2). Taken together, the high selectivity of the PCL-1 reporter system, its physiologically relevant low-micromolar detection limit, and its dose-dependent response are necessary features of a

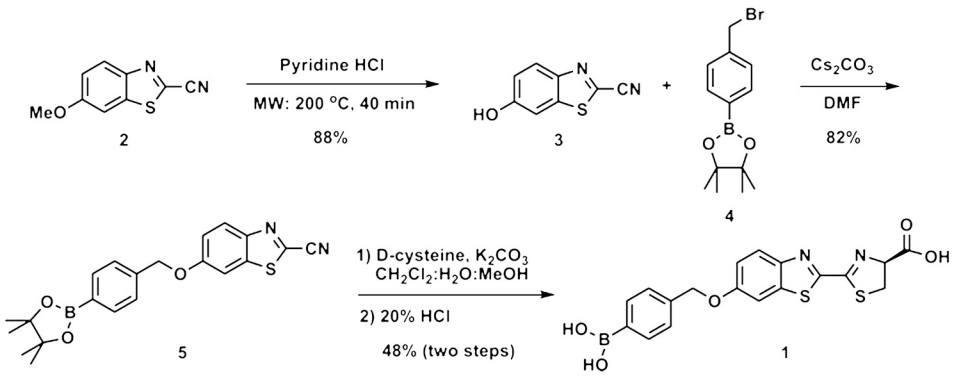

Scheme 1. Synthesis of PCL-1.

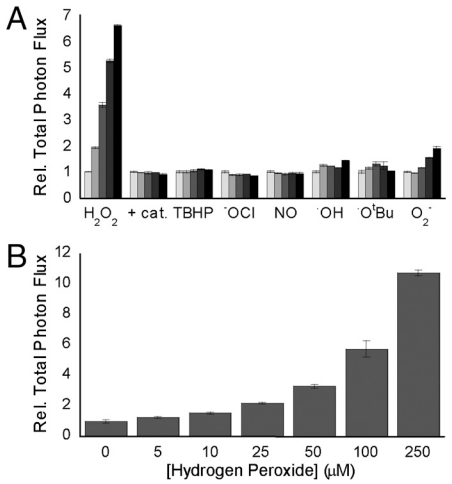

Fig. 2. Selective and concentration-dependent bioluminescent detection of H_2O_2 by PCL-1. (*A*) Total bioluminescent signal, integrated over 45 min, from PCL-1 (5 μM) alone (light gray bars) or incubated with various ROS (100 μM) or H_2O_2 (100 μM) and catalase (0.4 mg/mL) for 5, 20, 40, or 60 min. Signals were normalized to signal from PCL-1 in the absence of any ROS. (*B*) Total bioluminescent signal, integrated over 45 min, from 5 μM PCL-1 incubated for 1 h with increasing concentrations of H_2O_2 (0–250 μM). Signals were normalized to signal from PCL-1 in the absence of H_2O_2. To quantify free luciferin formation in *A* and *B*, 100 μg/mL luciferase in 50 mM Tris buffer with 10 mM $MgCl_2$, 0.1 mM $ZnCl_2$, and 2 mM ATP (pH 7.4) was added to the PCL-1 plus ROS solutions. Error bars are ±SD for two measurements (*A*) or three measurements (*B*).

practical probe that can detect changes in H_2O_2 levels in living systems in the presence of oxidative or reductive stimuli.

PCL-1 Visualizes Changes in H_2O_2 Levels in Living Cells by Bioluminescent Imaging. We next determined whether the performance of PCL-1 in aqueous solution translated to cell culture. Initial experiments using live-cell assays with exogenous H_2O_2 addition indicated that the presence of cells did not interfere with production of the H_2O_2-dependent bioluminescent signal and demonstrated a low, biologically relevant detection limit (2.5 μM) as well as a linear response to H_2O_2 *in cellulo* (Fig. S3) (2, 46). In subsequent experiments, to determine whether PCL-1 could detect endogenously produced H_2O_2 in living cells, we incubated LNCaP-luc cells with 500 μM paraquat for 24 h because previous work established that paraquat triggers elevations in intracellular H_2O_2 through disruption of the mitochondrial electron transport chain (47). Following paraquat stimulation, the LNCaP-luc cells were loaded with PCL-1 and the bioluminescent signal was measured. Paraquat-treated cells showed significantly ($p < 0.005$) higher levels of PCL-1 derived luminescence compared to unstimulated control cells (Fig. 3).

Because luciferin is a cell-permeable small molecule, three possible modes of action for PCL-1 are (*i*) reaction of this probe with H_2O_2 in the extracellular medium followed by cellular uptake of the free luciferin product, (*ii*) reaction of PCL-1 with intracellular H_2O_2 to generate luciferin within cells, or (*iii*) both of the above. To probe whether PCL-1 was reacting with H_2O_2 in the intra- and/or extracellular space, we added catalase to paraquat-stimulated cells as a cell-impermeable scavenger for extracellular H_2O_2 (48). We observed that the addition of catalase with paraquat causes a decrease in bioluminescent signal compared to addition of paraquat alone, but the signal did not decrease to the level of background signal of cells treated only with catalase in the absence of paraquat (Fig. 3). These data suggest that PCL-1 is capable of interacting with and detecting both extracellular and intracellular H_2O_2 pools. Moreover, because treatment with H_2O_2-scavenging catalase reduced the level of PCL-1 bioluminescence in cells compared to untreated specimens (Fig. 3),

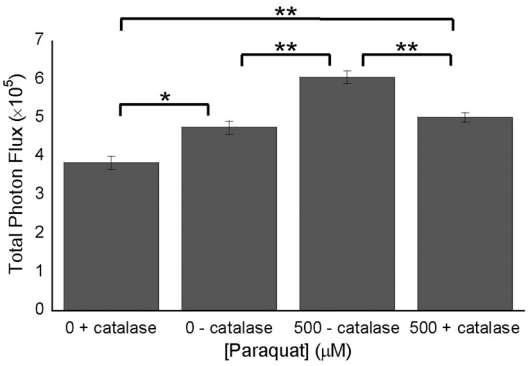

Fig. 3. Bioluminescent signal from PCL-1 added to LNCaP-luc cells. Total photon flux, integrated over 2 h, from LNCaP-luc cells incubated with paraquat (0 or 500 μM) for 24 h, followed by addition of PCL-1 (50 μM) ± catalase (1×10^4 U/L). Statistical analyses were performed with a two-tailed Student's *t* test. *$P < 0.05$, **$p < 0.005$ ($n = 3$), and error bars are ±SD.

the data also suggest that PCL-1 is sensitive enough to detect basal levels of H_2O_2 that are endogenously produced without addition of compounds that stimulate H_2O_2 production, highlighting the potential utility of PCL-1 for in vivo studies.

Molecular Imaging of H_2O_2 Fluxes in Living FVB-luc$^+$ Mice. We next sought to apply PCL-1 to molecular imaging of H_2O_2 in living animals. Initial studies utilized FVB-luc$^+$ mice (30) that ubiquitously express firefly luciferase along with exogenous peroxide addition. Several concentrations of H_2O_2 were injected into the i.p. cavity of unshaven FVB-luc$^+$ mice with subsequent i.p. injection of PCL-1, and the bioluminescent signal produced by these living animals was imaged in real-time using a CCD camera. Differences in bioluminescent signal from mice injected with different amounts of H_2O_2 can be detected within the first few minutes following injection, and monitoring of the integrated total photon flux for each mouse reveals a dose-dependent increase in signal as a function of the H_2O_2 concentration (Fig. 4). Although H_2O_2 clearly elevates the signal detected from PCL-1 in vivo, it has no impact on the signal produced by luciferin

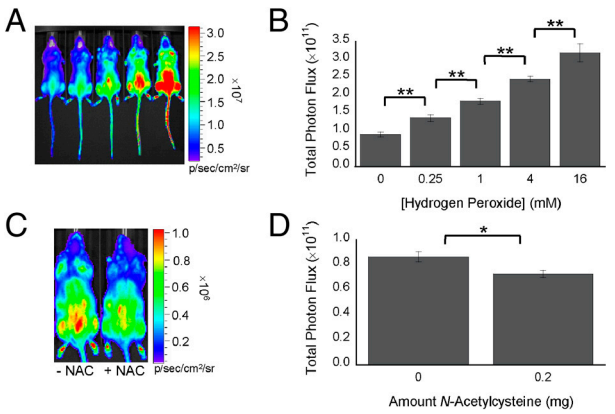

Fig. 4. Bioluminescent signal from PCL-1 in FVB-luc$^+$ mice. (*A*) Representative image (30 min postinjection) for mice injected with PCL-1 (i.p., 0.5 μmol in 50 μL of 1:1 DMSO:PBS) immediately prior to injection of H_2O_2 (i.p., 0, 0.37, 1.5, 6, or 24 mM, left to right, in 100 μL of PBS). (*B*) Total photon flux, integrated over 1 h, for mice injected with PCL-1 ± H_2O_2. H_2O_2 concentrations represent the H_2O_2 concentration in the i.p. cavity based on a total injection volume of 150 μL. Statistical analyses were performed with a two-tailed Student's *t* test. **$P < 0.005$ ($n = 5$) and error bars are ±SD. (*C*) Representative image (12 min postinjection) for mice injected with PCL-1 (i.p., 0.5 μmol in 50 μL of 1:1 DMSO:PBS) immediately following NAC (i.p., 0 or 0.2 mg in 100 μL PBS). (*D*) Total photon flux, integrated over 1 h, for mice injected with PCL-1 ± NAC. Statistical analyses were performed with a two-tailed Student's *t* test. *$P < 0.05$ ($n = 3$), and error bars are ±SD.

(Fig. S4). Interestingly, mice treated with only PCL-1 with no added peroxide also show modest but measurable bioluminescence throughout their bodies, suggesting that PCL-1 may be detecting basal levels of H_2O_2 produced in these living animals. To determine whether this emission signal was due in part to the detection of endogenous H_2O_2, we injected PCL-1 into unshaven FVB-luc$^+$ mice in the presence and absence of NAC, a commonly used antioxidant (49). We were pleased to observe that the NAC-treated animals exhibit a significantly reduced bioluminescent signal compared to vehicle control animals (Fig. 4). Control experiments in FVB-luc$^+$ mice with luciferin and NAC (Fig. S4) indicated that NAC has no effect on the bioluminescent production of photons in vivo, establishing that PCL-1 is sensitive enough to visualize basal levels of H_2O_2 in healthy, living animals without external stimulation of peroxide production.

Detection of Endogenous H_2O_2 in a Prostate Tumor Model. After establishing that the H_2O_2-mediated boronic acid deprotection of PCL-1 provides a selective and sensitive platform for real-time imaging of H_2O_2 in aqueous solution, in living cells, and in living mice, we sought to apply this bioluminescent reporter to studies of H_2O_2 physiology at an in vivo level. In the present study, we targeted the roles that H_2O_2 plays in the development and progression of cancer because recent reports suggest that tumor cells produce an elevated level of H_2O_2 compared to noncancerous cells and that this ROS increase is correlated with cancer cell growth and malignancy (50). Initial experiments focused on prostate cancer using androgen-sensitive prostate cancer cells (LNCaP). In dissociated cell culture, LNCaPs respond to testosterone by increasing their proliferation rate (51, 52) and elevating their ROS production (53), suggesting a link between oxidative stress and development of this disease. However, the probes previously used to detect oxidant production in LNCaPs do not selectively detect any particular ROS (53), and the environment that tumor cells experience in vivo is greatly different from dissociated cell culture conditions with variances in oxygen level, nutrient supply, and acidity (54). Thus, the application of tools to probe specific ROS molecules, like H_2O_2, in the context of a living animal is critical to elucidating the relationships between redox biology and cancer.

To study the production of H_2O_2 and stimulatory effects of testosterone in prostate cancer in living animals, we developed an i.p. LNCaP-luc tumor xenograft model in immunodeficient SCID hairless outbred (SHO) mice (Fig. S5). To determine the baseline levels of H_2O_2 generation in the tumors as well as alterations in H_2O_2 fluxes over 24 h, mice were injected with PCL-1 on day 1 and with PCL-1 and sesame oil, a vehicle used for all experiments, on day 2. No change in basal bioluminescent signal from the mice over the time course of the experiments was found (Fig. S6). We then moved on to test the effects of testosterone (in the form of testosterone propionate) on H_2O_2 production within the prostate cancer tumors. For these experiments, mice were injected with PCL-1 on day 1 and the baseline signal was measured. On day 2, the mice were injected with either testosterone propionate or empty vehicle, followed 1.5 h later by PCL-1. Mice treated with testosterone propionate showed a *ca.* 41% increase in total photon flux compared to vehicle control mice (Fig. 5). These data suggest that LNCaP-luc tumors produce elevated levels of H_2O_2 in vivo upon testosterone stimulation.

To ensure that the observed signal enhancement from testosterone stimulation of the LNCaP tumors was due to an increase in H_2O_2 production and not a result of nonspecific cellular and metabolic changes, we utilized a non-ROS responsive control compound, valeryl luciferin (Scheme S1) (55), in experiments identical to those outlined above for PCL-1. This esterase-cleavable luciferin was chosen as the control compound instead of firefly luciferin because the peak for signal produced by luciferin in LNCaP-luc cells, as opposed to many other luciferase transfected cells, is reached prior to the first imaging time point (<1 min after injection). In contrast, because valeryl luciferin requires cleavage of the valeryl ester prior to light production, the signal peak is shifted to later time points and can be detected within the time frame of the imaging experiments to ensure consistent quantitation of the bioluminescent signal. We observed no change in the bioluminescent signal from valeryl luciferin from day 1 to day 2 when mice were injected with vehicle alone or vehicle plus testosterone on the second day (Fig. S7). These results clearly indicate that testosterone does not alter the expression of firefly luciferase in the LNCaP-luc xenografts nor change the interactions between the luciferin derivatives and these tumors, which further validates that PCL-1 is imaging changes in tumor production of H_2O_2 upon testosterone stimulation.

In a final set of control experiments to confirm that PCL-1 was detecting a testosterone-triggered increase in tumor H_2O_2 production, we utilized NAC as a general chemical scavenger for H_2O_2. We performed these experiments by injecting mice on day 2 with testosterone propionate, followed 1.5 h later by serial administration of NAC and PCL-1. As shown in Fig. 5, NAC treatment causes a reduction in bioluminescent signal in testosterone-stimulated animals back to baseline levels, with light production comparable to vehicle control tumors. The collective data establish that androgen-sensitive prostate tumors respond to the proliferation signal of testosterone in vivo by elevating their production of H_2O_2.

Concluding Remarks

Hydrogen peroxide contributes to a diverse array of physiological and pathological events in living organisms, but there is an insufficient understanding of how local fluxes of this potent small-molecule oxidant can be beneficial or damaging to the entire an-

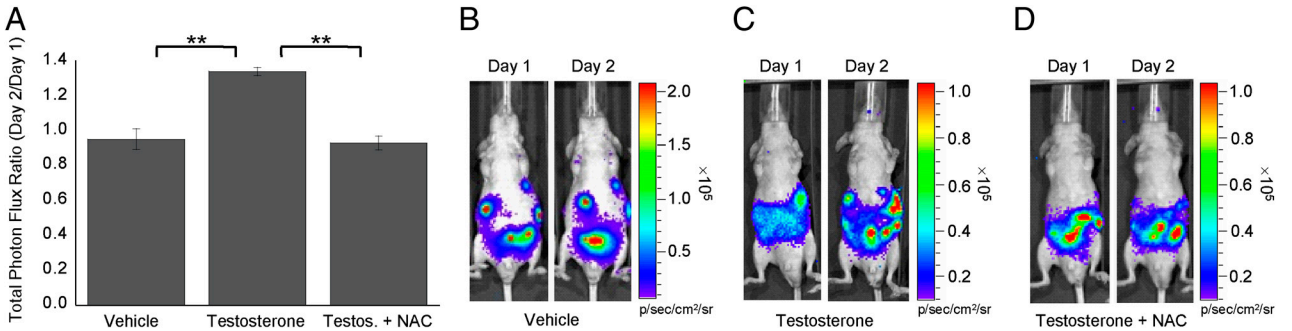

Fig. 5. Bioluminescent signal from SHO mice with LNCaP-luc tumors. (*A*) Ratios of total photon fluxes for mice injected with PCL-1 (i.p., 0.5 μmol in 50 μL of 1:1 DMSO:PBS) on day 1 and PCL-1 (i.p., 0.5 μmol in 50 μL of 1:1 DMSO:PBS) plus the vehicle (i.p., 50 μL of sesame oil), testosterone propionate (i.p., 3 mg in 50 μL of sesame oil), or testosterone propionate (i.p., 3 mg in 50 μL of sesame oil) and NAC (i.p., 0.2 mg in 100 μL of PBS) on day 2. Sesame oil and testosterone were injected 1.5 h prior to PCL-1 on day 2, and NAC was injected immediately prior to PCL-1 on day 2. Statistical analyses were performed with a two-tailed Student's *t* test. $^{**}P < 0.005$ ($n = 5$), and error bars are ±SD. Representative images from one mouse in each experiment are shown (*B–D*).

imal in stages of health, aging, injury, and disease. An emerging set of chemical tools for selective imaging of H_2O_2 at the cellular level continues to help elucidate the functions of this ROS in simplified model systems, but analogous approaches to probe such questions in vivo remain limited. In this study, we have presented a unique chemoselective reporter for real-time imaging of H_2O_2 produced in living animals. PCL-1 is a caged luciferin derivative that is activated upon selective cleavage of its H_2O_2-sensitive boronic acid group to generate free luciferin, which can then undergo reaction with luciferase to generate light through a bioluminescent reaction. We have shown that this reporter system is able to selectively detect H_2O_2 in a concentration-dependent manner in living cells and in living animals, demonstrating that the H_2O_2-mediated cleavage of boronic acids is a bioorthogonal reaction for H_2O_2 sensing that can reliably operate in vivo. In addition, live-mouse imaging experiments with the antioxidant NAC establish that PCL-1 is sensitive enough to visualize basal levels of H_2O_2 produced in vivo. Most notably, robust optical signals are observed in all areas of the mouse, including major organ systems like the brain, heart, liver, and intestines, presaging that animal models of various diseases and injury, such as heart disease, diabetes, stroke, and neurodegeneration, could be monitored using PCL-1.

We have demonstrated the utility of this imaging probe in an animal model of cancer through use of an androgen-sensitive prostate tumor xenograft model developed from the LNCaP-luc cell line. PCL-1 imaging reveals that these tumors trigger increased in vivo H_2O_2 production upon interaction with testosterone, and control experiments with the ROS-insensitive probe valeryl luciferin, as well as treatment with NAC, verify that PCL-1 is visualizing testosterone-induced changes in H_2O_2 fluxes.

In closing, our data shows that PCL-1 is a viable bioluminogenic probe for the detection of fluctuations in H_2O_2 produced in living animals. This small-molecule imaging agent is able to travel throughout the body of living mice and its redshifted luminescent reaction with luciferase allows for deep tissue signal penetration with an optical readout. Moreover, the use of PCL-1 does not require the death of the animal, which provides a significant advance in our ability to monitor disease progression in individual mice.

Materials and Methods

Materials and procedures for the synthesis of compounds, bioluminescent assays, and animal experiments are described in *SI Text*.

ACKNOWLEDGMENTS. We thank the Packard and Sloan Foundations (C.J.C.), Amgen (C.J.C.), Astra Zeneca (C.J.C.), Novartis (C.J.C.), and the National Institute of General Medical Sciences [National Institutes of Health GM 79465 (to C.J.C.) and National Institutes of Health GM 058867 (to C.R.B.)] for funding this work. C.J.C. and C.R.B. are Investigators with the Howard Hughes Medical Institute. We thank Christopher Contag (Stanford University, Stanford, CA) for his generous gift of LNCaP-luc cells and FVB-luc$^+$ mice, as well as Ann Fischer at the UCB Tissue Culture Facility for her help with culturing the LNCaP-luc cells.

1. Rhee SG (2006) H_2O_2, a necessary evil for cell signaling. *Science* 312:1882–1883.
2. Stone JR, Yang S (2006) Hydrogen peroxide: A signaling messenger. *Antioxid Redox Signaling* 8:243–270.
3. D'AutrEaux B, Toledano MB (2007) ROS as signaling molecules: Mechanisms that generate specificity in ROS homeostasis. *Nat Rev Mol Cell Biol* 8:813–824.
4. Miller EW, Chang CJ (2007) Fluorescent probes for nitric oxide and hydrogen peroxide in cell signaling. *Curr Opin Chem Biol* 11:620–625.
5. Winterbourn CC (2008) Reconciling the chemistry and biology of reactive oxygen species. *Nat Chem Biol* 4:278–286.
6. Paulsen CE, Carroll KS (2010) Orchestrating redox signaling networks through regulatory cysteine switches. *ACS Chem Biol* 5:47–62.
7. Finkel T, Serrano M, Blasco MA (2007) The common biology of cancer and ageing. *Nature* 448:767–774.
8. Rossi DJ, Jamieson CHM, Weissman IL (2008) Stem cells and the pathways to aging and cancer. *Cell* 132:681–696.
9. Houstis N, Rosen ED, Lander ES (2006) Reactive oxygen species have a causal role in multiple forms of insulin resistance. *Nature* 440:944–948.
10. Jay D, Hitomi H, Griendling KK (2006) Oxidative stress and diabetic cardiovascular complications. *Free Radical Biol Med* 40:183–192.
11. Looi YH, et al. (2008) Involvement of Nox2 NADPH oxidase in adverse cardiac remodeling after myocardial infarction. *Hypertension* 51:319–325.
12. Ushio-Fukai M, Urao N (2009) Novel role of NADPH oxidase in angiogenesis and stem/progenitor cell function. *Antioxid Redox Signaling* 11:2517–2533.
13. Barnham KJ, Masters CL, Bush AI (2004) Neurodegenerative diseases and oxidative stress. *Nat Rev Drug Discovery* 3:205–214.
14. Lin MT, Beal MF (2006) Mitochondrial dysfunction and oxidative stress in neurodegenerative diseases. *Nature* 443:787–795.
15. Maeda H, et al. (2004) Fluorescent probes for hydrogen peroxide based on a non-oxidative mechanism. *Angew Chem, Int Ed* 43:2389–2391.
16. Chang MCY, Pralle A, Isacoff EY, Chang CJ (2004) A selective, cell-permeable optical probe for hydrogen peroxide in living cells. *J Am Chem Soc* 126:15392–15393.
17. Soh N (2006) Recent advances in fluorescent probes for the detection of reactive oxygen species. *Anal Bioanal Chem* 386:532–543.
18. Miller EW, Tulyathan O, Isacoff EY, Chang CJ (2007) Molecular imaging of hydrogen peroxide produced for cell signaling. *Nat Chem Biol* 3:263–267.
19. Dickinson BC, Chang CJ (2008) A targetable fluorescent probe for imaging hydrogen peroxide in the mitochondria of living cells. *J Am Chem Soc* 130:9638–9639.
20. Srikun D, Albers AE, Nam CI, Iavarone AT, Chang CJ (2010) Organelle-targetable fluorescent probes for imaging hydrogen peroxide in living cells vie SNAP-tag protein labeling. *J Am Chem Soc* 132:4455–4465.
21. Dickinson BC, Huynh C, Chang CJ (2010) A palette of fluorescent probes with varying emission colors for imaging hydrogen peroxide signaling in living cells. *J Am Chem Soc* 132:5906–5915.
22. Belousov VV, et al. (2006) Genetically encoded fluorescent indicator for intracellular hydrogen peroxide. *Nat Methods* 3:281–286.
23. Lee D, et al. (2007) *In vivo* imaging of hydrogen peroxide with chemiluminescent nanoparticles. *Nat Mater* 6:765–769.
24. Seliger HH, McElroy WD (1960) Spectral emission and quantum yield of firefly bioluminescence. *Arch Biochem Biophys* 88:136–141.
25. Ando Y, et al. (2008) Firefly bioluminescence quantum yield and color change by pH-sensitive green emission. *Nat Photonics* 2:44–47.
26. Zhao H, et al. (2005) Emission spectra of bioluminescent reporters and interaction with mammalian tissue determine the sensitivity of detection *in vivo*. *J Biomed Opt* 10:041210.
27. Mezzanotte L, et al. (2010) *In vivo* bioluminescence imaging of murine xenograft cancer models with a red-shifted thermostable luciferase. *Mol Imaging Biol* 12:406–414.
28. Craig FF, Simmons AC, Watmore D, McCapra F, White MRH (1991) Membrane-permeable luciferin esters for assay of firefly luciferase in live intact cells. *Biochem J* 276:637–641.
29. Prescher JA, Contag CH (2010) Guided by the light: Visualizing biomolecular processes in living animals with bioluminescence. *Curr Opin Chem Biol* 14:80–89.
30. Cao YA, et al. (2004) Shifting foci of hematopoiesis during reconstitution from single stem cells. *Proc Natl Acad Sci USA* 101:221–226.
31. Berger F, Paulmurugan R, Bhaumik S, Gambhir S (2008) Uptake kinetics and biodistribution of ^{14}C-D-luciferin—a radiolabeled substrate for the firefly luciferase catalyzed bioluminescence reaction: impact on bioluminescence based reporter gene imaging. *Eur J Nucl Med Mol Imaging* 35:2275–2285.
32. Kheirolomoom A, et al. (2010) Enhanced *in vivo* bioluminescence imaging using liposomal luciferin delivery system. *J Controlled Release* 141:128–136.
33. Geiger R, Schneider E, Wallenfels K, Miska W (1992) A new ultrasensitive bioluminogenic enzyme substrate for β-galactosidase. *Biol Chem Hoppe-Seyler* 373:1187–1191.
34. O'Brien MA, et al. (2005) Homogeneous, bioluminescent protease assays: Caspase-3 as a model. *J Biomol Screening* 10:137–148.
35. Wehrman TS, von Dogenfeld G, Krutzik PO, Nolan GP, Blau HM (2006) Luminescent imaging of β-galactosidase activity in living subjects using sequential reporter-enzyme luminescence. *Nat Methods* 3:295–301.
36. Yao H, So M-k, Rao J (2007) A bioluminogenic substrate for *in vivo* imaging of β-lactamase activity. *Angew Chem, Int Ed* 46:7031–7034.
37. Zhou W, et al. (2008) Self-cleavable bioluminogenic luciferin phosphates as alkaline phosphatase reporters. *ChemBioChem* 9:714–718.
38. Dragulescu-Andrasi A, Liang G, Rao J (2009) *In vivo* bioluminescence imaging of furin acitivity in breast cancer cells using bioluminogenic substrates. *Bioconjugate Chem* 20:1660–1666.
39. Wender PA, et al. (2007) Real-time analysis of uptake and bioactivatable cleavage of luciferin-transporter conjugates in transgenic reporter mice. *Proc Natl Acad Sci USA* 104:10340–10345.
40. Denburg JL, Lee RT, McElroy WD (1969) Substrate-binding properties of firefly luciferase: I. Luciferin-binding site. *Arch Biochem Biophys* 134:381–394.
41. Srikun D, Miller EW, Domaille DW, Chang CJ (2008) An ICT-based approach to ratiometric fluorescence imaging of hydrogen peroxide produced in living cells. *J Am Chem Soc* 130:4596–4597.
42. Albers AE, Dickinson BC, Miller EW, Chang CJ (2008) A red-emitting naphthofluorescein-based fluorescent probe for selective detection of hydrogen peroxide in living cells. *Bioorg Med Chem Lett* 18:5948–5950.
43. Carl PL, Chakravarty PK, Katzenellenbogen JA (1981) A novel linkage applicable in prodrug design. *J Med Chem* 24:479–480.
44. Andrianomenjanahary S, et al. (1992) Synthesis of novel targeted pro-prodrugs of anthracyclines potentially activated by a monoclonal antibody galactosidase conjugate. *Bioorg Med Chem Lett* 2:1093–1096.

45. Florent J-C, et al. (1998) Prodrugs of anthracyclines for use in antibody-directed enzyme prodrug therapy. *J Med Chem* 41:3572–3581.
46. Kulagina NV, Michael AC (2003) Monitoring hydrogen peroxide in the extracellular space of the brain with amperometric microsensors. *Anal Chem* 75:4875–4881.
47. Castello PR, Drechsel DA, Patel M (2007) Mitochondria are a major source of paraquat-induced reactive oxygen species production in the brain. *J Biol Chem* 282:14186–14193.
48. Weissenberg A, et al. (2010) Reactive oxygen species as mediators of membrane-dependent signaling induced by ultrafine particles. *Free Radical Biol Med* 49:597–605.
49. Winterbourn CC, Metodiewa D (1999) Reactivity of biologically important thiol compounds with superoxide and hydrogen peroxide. *Free Radical Biol Med* 27:322–328.
50. Verschoor ML, Wilson LA, Singh G (2010) Mechanisms associated with mitochondrial-generated reactive oxygen species in cancer. *Can J Physiol Pharmacol* 88:204–219.
51. Antognelli C, et al. (2007) Alteration of glyoxalases gene expression in response to testosterone in LNCaP and PC3 human prostate cancer cells. *Cancer Biol Ther* 6:1880–1888.
52. Jennbacken K, et al. (2009) The prostatic environment suppresses growth of androgen-independent prostate cancer xenografts: An effect influenced by testosterone. *Prostate* 69:1164–1175.
53. Sun X-Y, Donald SP, Phang JM (2001) Testosterone and prostate specific antigen stimulate generation of reactive oxygen species in prostate cancer cells. *Carcinogenesis* 22:1775–1780.
54. Stewart GD, et al. (2009) The relevance of a hypoxic tumour microenvironment in prostate cancer. *BJU Int* 105:8–13.
55. Toya Y, et al. (1992) Improved synthetic methods of firefly luciferin derivatives for use in bioluminescent analysis of hydrolytic enzymes; carboxylic esterase and alkaline phosphatase. *Bull Chem Soc Jpn* 65:2604–2610.